

Ensemble radar precipitation estimation — a new topic on the radar horizon

Urs Germann¹, M Berenguer^{2,3}, D Sempere-Torres², and G Salvadè⁴

¹MeteoSwiss, CH-6605 Locarno-Monti (Switzerland).

²GRAHI, Universitat Politècnica de Catalunya (Spain).

³McGill University, Montréal (Canada).

⁴Istituto Scienze della Terra, Lugano (Switzerland).

Abstract. The uncertainty in radar precipitation estimates is the superposition of errors of many different error sources such as ground clutter, hardware instability, beam shielding, beam broadening, variability in the hydrometeor phase and size distribution, and signal attenuation by water on the radome or in the atmosphere. In the past decade MeteoSwiss developed and implemented a series of sophisticated algorithms to correct for several of the above errors. In spite of significant improvements, for hydrological applications the residual uncertainty is still relatively large.

An elegant way to express this residual uncertainty is the generation of an ensemble of radar precipitation fields using stochastic simulation and knowledge of errors. The ensemble represents the uncertainty in radar precipitation estimates by introducing perturbations with the correct space-time variances and auto-covariances. The variance and auto-covariance of errors strongly depend on the location, in particular in a mountainous region such as Switzerland. This dependence on location needs to be taken into account in the stochastic simulation. The paper presents a prototype ensemble generator that allows full flexibility with respect to the radar error structure.

1 Introduction

A recent publication (Germann et al., 2006) presents the Swiss approach for operational radar precipitation estimation in a mountainous region and a systematic objective verification based on a 7-year radar-gauge comparison. The continuous innovations in the precipitation estimation algorithms resulted in a significant reduction of radar errors. However, for hydrological applications the residual uncertainty is still relatively large, and needs to be taken into account when using radar measurements in a routine manner.

Correspondence to: Urs Germann
(urs.germann@meteoswiss.ch)

This paper explores the novel idea of generating ensembles of radar precipitation estimates. The radar precipitation field is perturbed with correlated random noise, which represents the residual space-time uncertainty in the radar estimates. The perturbation fields are generated by combining stochastic simulation techniques with detailed knowledge on the space-time variance and auto-covariance of radar errors.

Principally, there are two different approaches to determine the uncertainty of radar precipitation estimates:

1. Use an independent source of information such as rain gauges as a reference, and take the difference between the radar and the reference as an estimate of total uncertainty in radar estimates (e.g. Germann et al., 2006).
2. Examine all relevant sources of uncertainty separately by simulating the errors with conceptual physical models and/or experimental data (e.g. Bellon et al., 2005; Lee and Zawadzki, 2005), and calculate superposition of errors.

The advantage of the first approach lies in its simplicity and the fact that it directly gives an estimate of the total uncertainty in case we have several sources of error of the same order of magnitude. Of course, this can not resolve variability at scales smaller than the spacing between gauges. The second approach provides more insight into the origin and characteristics of errors, but may require a lot of work yet to be done. The focus of this explorative study is on our prototype ensemble generator. We therefore decided to follow the first approach and use radar-gauge agreement as a first estimate of total residual uncertainty in radar precipitation estimates.

Section 2 summarises recent progress in operational radar precipitation estimation in Switzerland. Section 3 provides a first look at the auto-correlation of residual radar errors, which is mandatory input for the ensemble generator. In section 4 we present our prototype ensemble generator based

on a stochastic simulation technique. First results for a 2'800 km² test catchment in the Southern Alps are presented in Section 5. In section 6 we provide some preliminary conclusions.

2 Progress in radar precipitation estimation in a mountainous region

This section briefly presents the results of an objective large sample verification of operational radar precipitation estimates in the Swiss Alps. For definitions and a detailed description of both the approach and the long-term verification the reader is referred to Germann et al. (2006).

The verification is based on a comparison of daily precipitation as observed by a dense gauge network and corresponding radar estimates of a 7-year period. There is no subjective selection of events or gauges. All days of the whole period and gauges more or less evenly spread over all of Switzerland were taken into account. We thus get an honest overall assessment of radar estimates over the whole territory including all types of precipitation.

The modifications in the radar precipitation estimation procedures are made one at a time, usually during the winter months. Comparison of the accuracy of radar estimates in the summer half year thus allows to evaluate step by step the improvements achieved by the individual algorithm changes. Particular attention was paid to the definition of robust and meaningful quality parameters. The probability of detection (POD), false alarm ratio (FAR), critical success index (CSI), and equitable threat score (ETS) for a threshold of 0.3 mm per day describe the ability of the radar to distinguish between precipitation and no precipitation. To assess the ability of the radar to get the correct precipitation *amounts* we use the overall radar-gauge ratio (bias), a robust estimator of the standard deviation expressed in dB or as a factor (scatter), the amount of totally missed precipitation as a fraction of total precipitation (mP), and, the amount of falsely detected precipitation as a fraction of total precipitation (fP).

For the summer half year 2004 we get a negligible overall bias of -1.3%, and a scatter of 2.3 dB which corresponds to a factor of 1.7. The POD, FAR, CSI and ETS are 90, 15, 78 and 63%, respectively. The somewhat low POD and high FAR look less dramatic if we determine the corresponding amount of precipitation as a fraction of total precipitation: mP and fP, which are 2 and 0.1%, respectively. The results for 2004 include the local bias correction procedure developed in the VOLTAIRE project. The same numbers for summer 1997 are -43% bias, 4.0 dB scatter, 84% POD, 34% FAR, 59% CSI, 40% ETS, 5% mP, and 0.1% fP.

Figure 1 depicts scatter, POD, FAR, mP and fP for 9 sub-regions. The figure clearly reveals the strong dependence of radar uncertainty on the geographic location. The bias for these 9 subregions ranges between -19% and 13% (not shown).

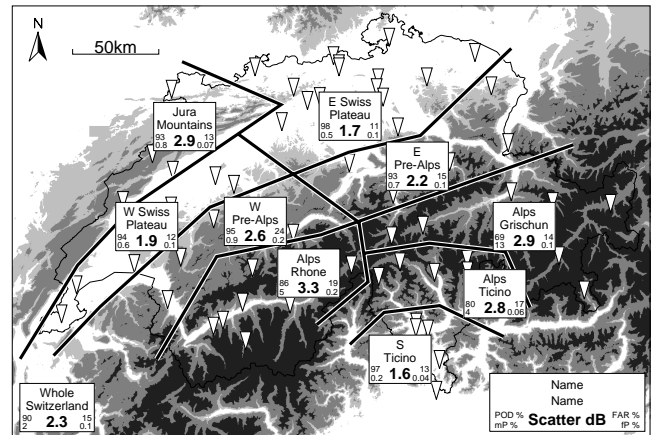


Fig. 1. Geographic dependence of uncertainty of radar precipitation estimates over Switzerland for summer 2004 after correction of local bias. Values are based on radar-gauge comparison at 58 gauge locations (triangles).

3 A glimpse on the auto-correlation of radar uncertainty

The systematic geographic dependence shown in Fig. 1 reflects the strong relation between radar errors and factors such as distance from the antenna, radar horizon and precipitation regimes. In other words, the uncertainty in radar precipitation estimates strongly varies as a function of location. This space-dependence needs to be taken into account when generating an ensemble of radar precipitation fields.

The next question is, to what extent is an error at a given location and time correlated with the error at a *different* location and time. Hydrologic applications typically combine many radar pixels such as a time series of all measurements over a given catchment. The sensitivity of the hydrologic model to radar errors then strongly depends on the auto-covariance of radar errors. If radar errors are completely uncorrelated in space and time the impact on the output of the hydrologic model will be relatively small, as errors average out when integrated in time and space. If, however, radar errors exhibit high auto-correlation we have to expect a large impact on the hydrologic simulation.

To get a first idea of the auto-correlation we pool hourly radar-gauge pairs of summer half year of 2003-2005, and calculate correlation between errors at a given gauge location with errors at all other gauge locations. Errors are weighted with the amount of precipitation. This analysis is limited to auto-correlation in space. In a next step we will also look at auto-correlation in time, and how this depends on location. Figures 2 and 3 show the results for two gauge locations, one in a valley in the Alps (Chur) and one in the flat Swiss plateau close to Zurich (Reckenholz). The location in the Alps exhibits high correlation with many locations in the Alpine

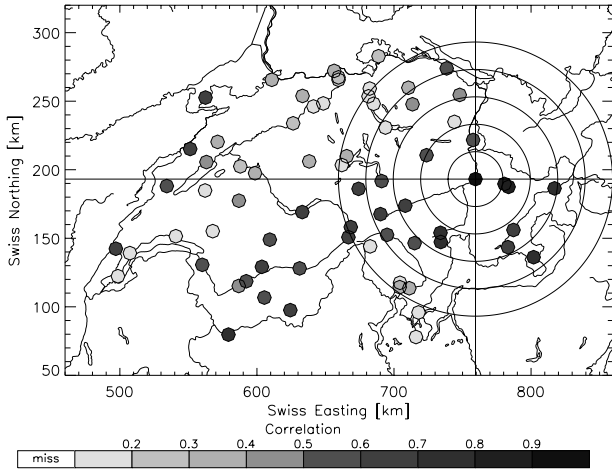


Fig. 2. Auto-correlation of radar errors for gauge location Chur in a valley in the eastern Swiss Alps. The grey-shaded circles show the correlation of radar errors over Chur with errors at all other gauge locations in whole Switzerland. Radar errors are evaluated for hourly time steps of whole summer half year of 2003-2005. The rings indicate distance from Chur in 20 km intervals up to 100 km.

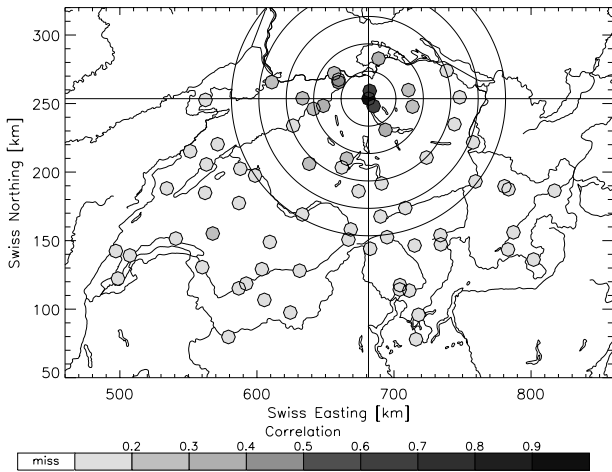


Fig. 3. Same as Fig. 2 for gauge location Reckenholz, close to Zurich in the relatively flat Swiss plateau.

bow and the Jura mountains in western Switzerland, while the correlation for the location in the Swiss plateau rapidly decreases with distance and shows no remote correlation at all. This again illustrates the strong relation between radar errors and “geographic” factors such as distance from the antenna, radar horizon and precipitation regimes. To model the correlation pattern of Chur with a simple distance-dependent isotropic or anisotropic variogram approach would be unsatisfactory.

4 Ensemble generator

The idea of the radar ensemble is to generate perturbation fields by means of stochastic simulation, and to add the perturbation to the original radar precipitation fields. As most of the radar errors are multiplicative we decided to generate and add perturbations in the logarithmic domain, that is $\text{dB}(\mathbf{R})$, the logarithm of precipitation rates

$$\log \mathbf{R}'_i = \log \mathbf{R}_0 + \delta_i \quad (1)$$

where \mathbf{R}'_i is radar precipitation ensemble member i , \mathbf{R}_0 is original radar precipitation field, and, δ_i is perturbation vector for ensemble member i .

Errors are auto-correlated both in time and space. In order to limit complexity and size of this explorative study we only model perturbation in space and ignore time. That is, we produce ensembles for a single given time step. The design of the presented ensemble generator, however, is such that it can easily be extended to whole time series of images.

How do we generate a number of perturbation vectors δ_i with given mean, variance and auto-covariance? If the spatial decorrelation of errors does not depend on location we can produce white gaussian random noise and introduce the desired correlation structure by imposing a given slope in the power spectrum using Fourier transform. The preliminary results presented in the previous sections, however, show a strong dependence of error structure on the geographic location. The simple approach via the power spectrum would impose the same error structure independently of location, and is thus not much convincing in a mountainous context. Future work has to show to what extent the power spectrum approach may be relaxed to be more flexible.

We decided to test a different technique which provides full flexibility with respect to the space-time dependence of the mean, variance and auto-covariance. It is based on the Cholesky decomposition (e.g. Press et al., 1992)

$$\mathbf{C} = \mathbf{L}\mathbf{L}^T \quad (2)$$

of a positive-definite symmetric matrix \mathbf{C} , see e.g. Ripley (1987). For better numerical stability we use the modified Cholesky algorithm proposed by Gill and Murray in 1974 (see Gill et al., 1981). The perturbation vector δ is generated as follows

$$\delta_i = \boldsymbol{\mu} + \mathbf{L}\boldsymbol{\epsilon}_i \quad (3)$$

where $\boldsymbol{\mu}$ is mean error vector, \mathbf{L} is the lower-triangular matrix as obtained by Cholesky decomposition of \mathbf{C} (the variance-covariance matrix of radar errors), and $\boldsymbol{\epsilon}_i$ is random white noise.

5 First results

For a proof of concept of the approach outlined in the previous section we selected a 2'800 km² catchment in the southern Alps (Fig. 4). Radar-gauge data pairs for daily precipita-

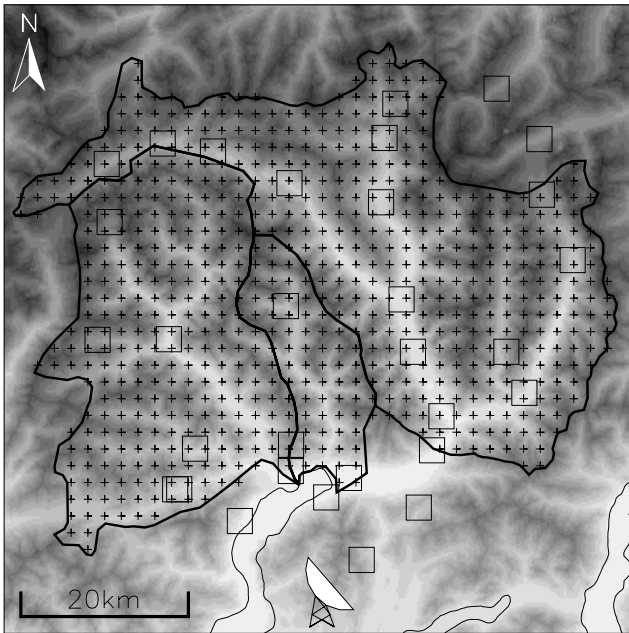


Fig. 4. Testbed with 2'800 km² catchment to the north of MeteoSwiss radar on Monte Lema (1625 m). The small crosses show the 697 radar pixels within the catchment, and the boxes indicate the locations of the 31 gauges used to determine the mean error vector and the error variance-covariance matrix. Grey shades show terrain height. The catchment includes several mountain peaks above 3000 m above sea level. The lake at the outlet of the catchment is at 200 m above sea level.

tion during summer half year 2005 at 31 gauge locations in or close to the catchment is used to determine the mean error μ , and the error variance-covariance matrix C . The resulting μ and C are in good agreement with the experience from previous analyses (e.g. Germann et al., 2006). An example of the perturbation vector δ of a single ensemble member is depicted in Fig. 5.

6 Conclusions

The preliminary results of this study proof the feasibility of the presented approach. The ensemble generator based on Cholesky decomposition provides full flexibility regarding the mean error and the error variance-covariance matrix, a clear advantage in complex terrain where radar errors exhibit strong dependence on the geographic location.

Future steps are 1) to generate ensembles for periods shorter than 24 hours, 2) to extend the ensemble generator to time including error auto-covariance in time, 3) conditioning of the stochastic generation of perturbations, 4) to develop a technique to select relevant members from a large ensemble (this depends on the sensitivity of the application to radar errors), and 5) make first real tests in a hydrological context

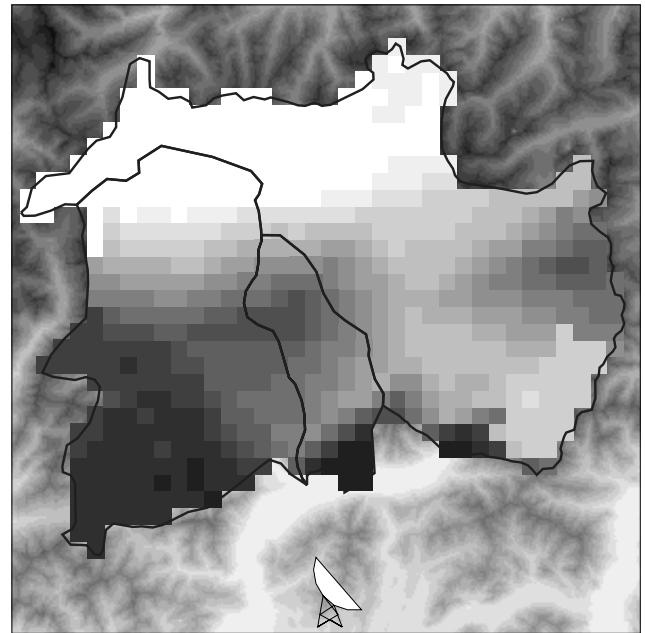


Fig. 5. Example of perturbation vector δ . Grey shades indicate δ ranging from “adding 4 dB” (white) to “subtracting 2 dB” (black). Same domain as Fig. 4.

in the WMO-WWRP forecast demonstration project MAP D-PHASE of the Mesoscale Alpine Programme (MAP), see Rotach (2004), a target area of which is the Lago Maggiore region next to the MeteoSwiss radar Monte Lema.

Acknowledgements. This work is part of the European concerted research action COST-731 and was stimulated by discussions with several colleagues, in particular with Isztar Zawadzki, Xavi Llorc, Eduardo Cassiraga, Rafael Sanchez-Diezma, Carlos Velasco-Forero, María Franco, Alan Seed and Thomas Einfalt.

References

- Bellon, A., Lee, G., and Zawadzki, I.: Error Statistics of VPR Corrections in Stratiform Precipitation, *JAM*, 44, 998–1015, 2005.
- Germann, U., Galli, G., Boscacci, M., and Bolliger, M.: Radar precipitation measurement in a mountainous region, *Q. J. R. Meteorol. Soc.*, 132, scheduled for July issue, 2006.
- Gill, P. E., Murray, W., and Wright, M. H.: *Practical Optimization*, Academic Press, 401 pp, 1981.
- Lee, G.-W. and Zawadzki, I.: Variability of Drop Size Distributions: Time-Scale Dependence of the Variability and its Effects on Rain Estimation, *J. Appl. Meteor.*, 44, 241–255, 2005.
- Press, W. H. et al.: *Numerical Recipes in C — The Art of Scientific Computing*, Cambridge University Press, 1992.
- Ripley, B. D.: *Stochastic simulation*, Wiley series in probability and mathematical statistics, John Wiley & Sons, 237 pp, 1987.
- Rotach, M.: The upcoming MAP Forecast Demonstration Project (FDP), *MAP Newsletter*, 19, 6–8, available from MeteoSwiss, Krähbühlstr. 58, CH-8044 Zürich, 2004.